Supplemental Material

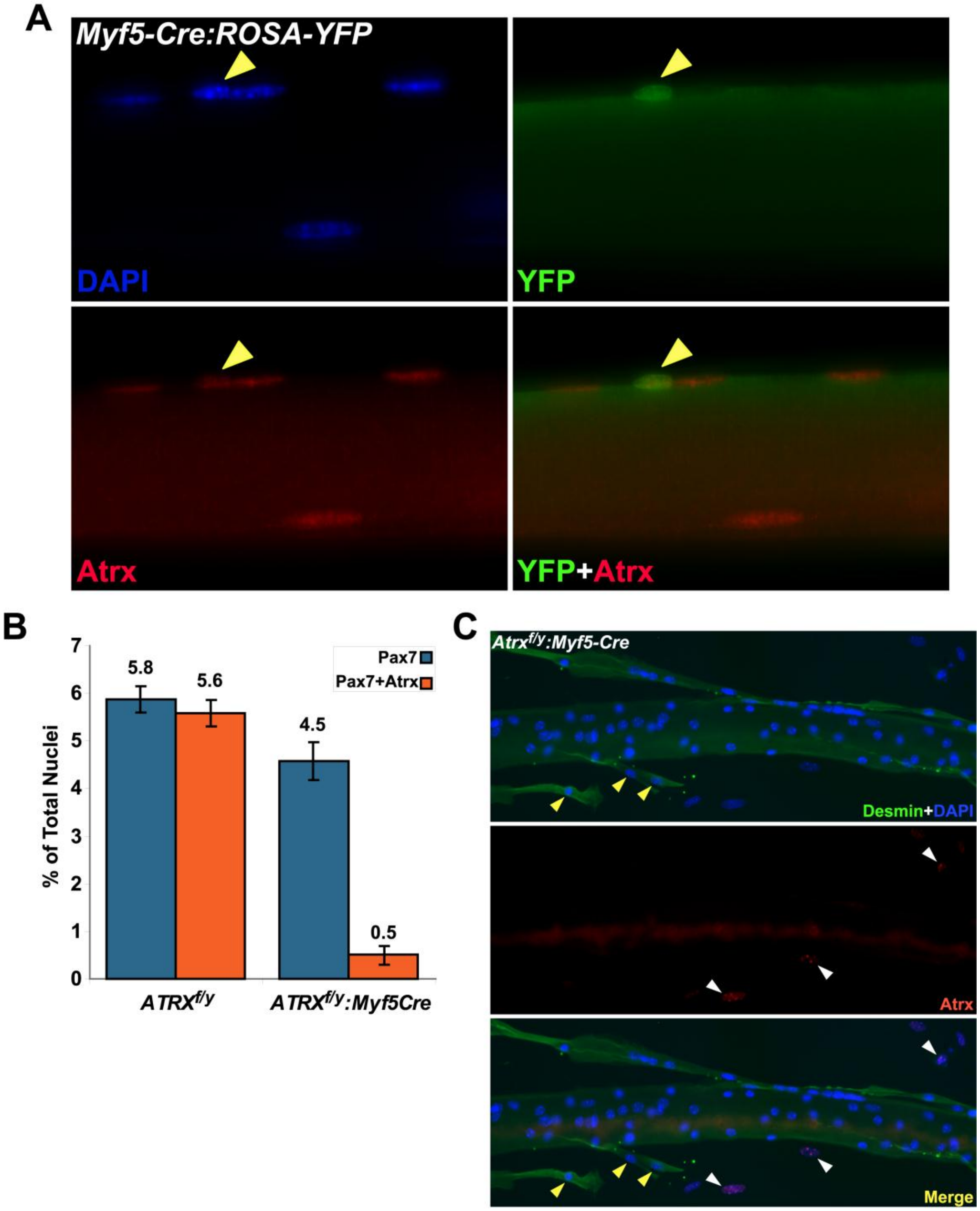

Figure S1.(A) Immuno-staining of freshly isolated *Myf5-Cre:ROSA-YFP* fiber (B) Satellite cell enumeration in WT and cKO mice from resting hind limb muscles. Bulk hind limb muscles were dissociated and immuno-stained for Pax7 and Atrx. Values represent percent total stained ± 95% CI (*Atrx*$^{f/y}$(n=4); 5834 total nuclei) (*Atrx*$^{f/y}$*:Myf5-Cre*(n=3); 2957 total nuclei) (C) Muscle specific inactivation of *Atrx* in *Atrx*$^{f/y}$*:Myf5-Cre* muscle fiber. Single muscle fiber was cultured for 6 days and immuno-stained for skeletal muscle intermediate filament protein Desmin and Atrx. Atrx is not expressed in all Desmin positive nuclei (yellow arrowheads) due to the muscle specific expression of *Myf5-Cre*. White arrowheads indicate non-myogenic fibroblastic nuclei that retain expression of Atrx. Original magnifications in A, 630x; C, 400x.

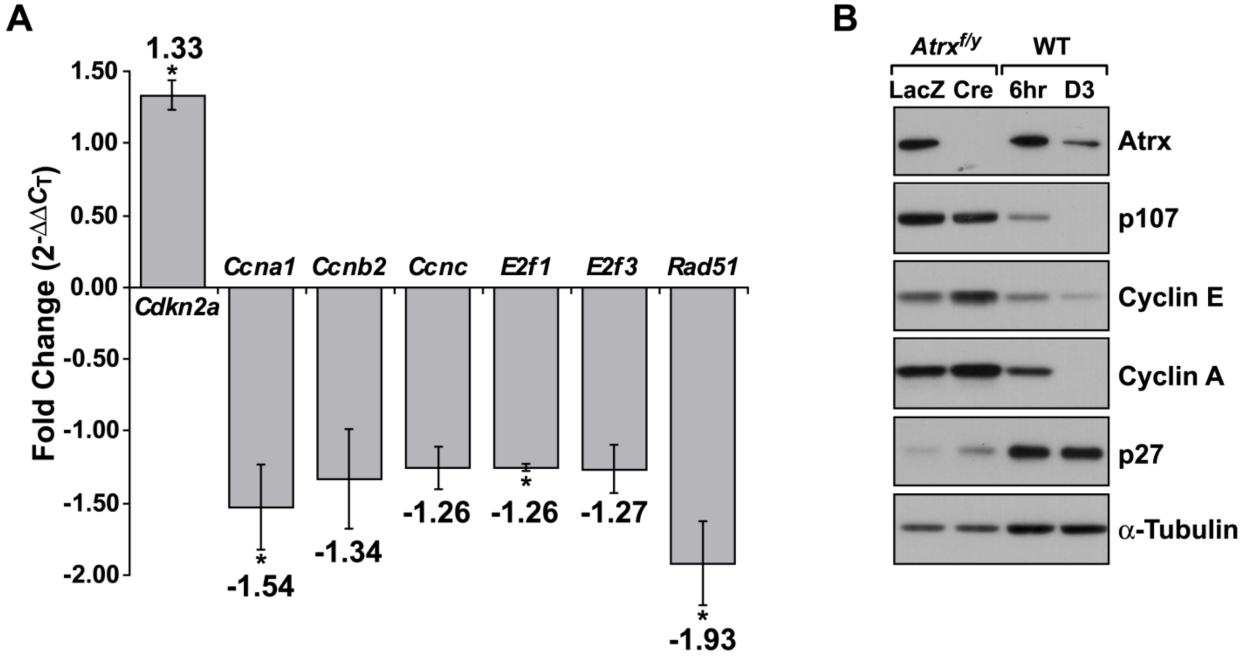

Figure S2. Expression changes of cell cycle regulators in Atrx depleted myoblasts. (A) RT QPCR analysis of cell cycle regulators. Normalized critical threshold (ΔC_T) values for Ad-LacZ and Ad-Cre infected myoblasts were calculated and converted to fold change by comparative C_T method (fold change = $2^{-\Delta\Delta C_T}$), where $\Delta\Delta C_T = [\Delta C_T^{\text{Ad-Cre}}] - [\Delta C_T^{\text{Ad-LacZ}}]$; fold change values < 1 were represented as –[1/(fold change < 1)]. Values represent mean fold-change ± SEM (n=3). (*) $p<0.05$ by t-test. (B) Western blot analysis of S-phase cell cycle regulatory proteins in *Atrx*$^{f/y}$ myoblasts infected with adenovirus expressing LacZ or Cre recombinase. Cell cycle withdrawal was induced in wildtype (WT) myoblasts at early (6hr) and late (D3) differentiation time points. Immuno-blots were probed with antibodies specific Atrx, p107, Cyclin E, Cyclin A, p27, and α-tubulin for loading control.

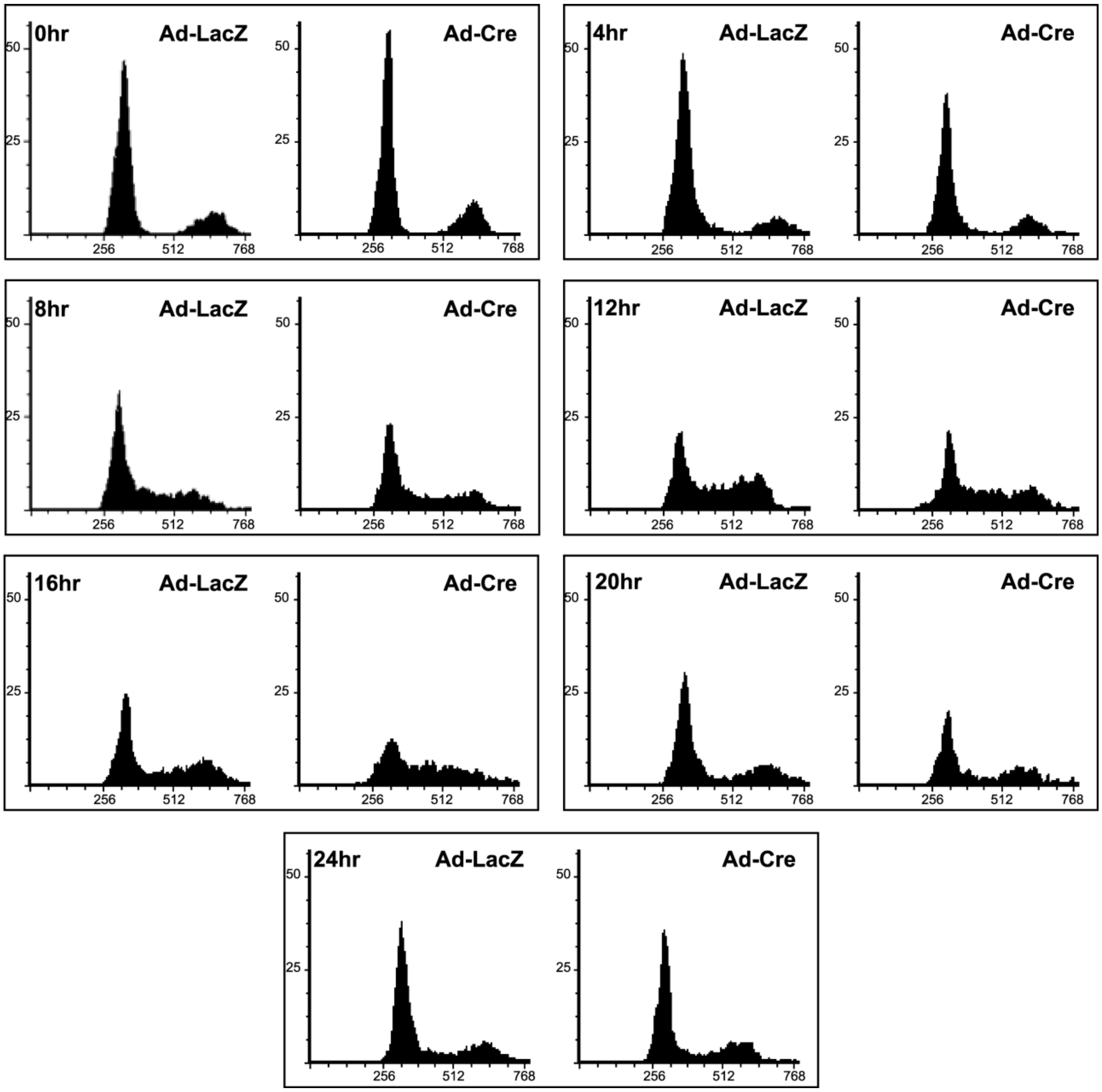

Figure S3. Flow cytometry cell cycle progression analysis of the BrdU negative population from Ad-LacZ and Ad-Cre infected *Atrx*$^{f/y}$ myoblasts. Histograms represent the relative proportion of BrdU negative cells with respect to propidium iodide (PI) labelled DNA content following a BrdU pulse.

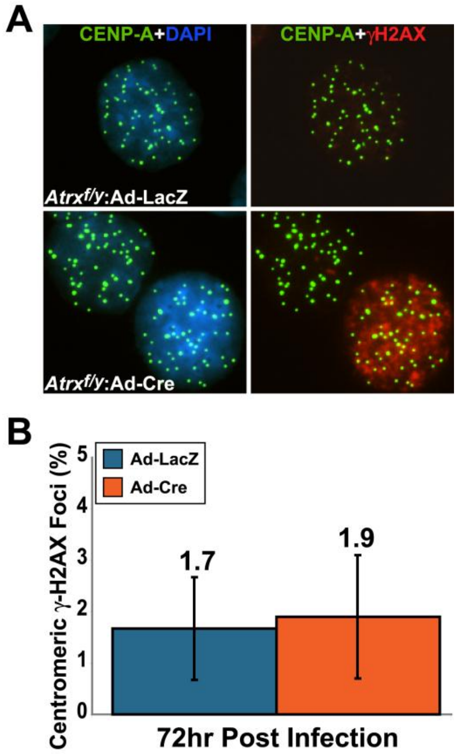

Figure S4. Depletion of Atrx does not increase DNA damage response at centromeres. (A) Double immuno-fluorescent micrograph for the centromeric histone variant Cenp-A and γ-H2AX in Ad-LacZ and Ad-Cre infected *Atrx*$^{f/y}$ myoblasts. (B) Percentage of total nuclei with >2 CENP-A foci with γ-H2AX labelling in Ad-LacZ and Ad-Cre infected *Atrx*$^{f/y}$ myoblasts. Values represent percent total ± 95% CI (*Atrx*$^{f/y}$:Ad-LacZ (n=3); 597 total nuclei) (*Atrx*$^{f/y}$:Ad-Cre (n=3); 472 total nuclei). Original magnification in A, 630x.

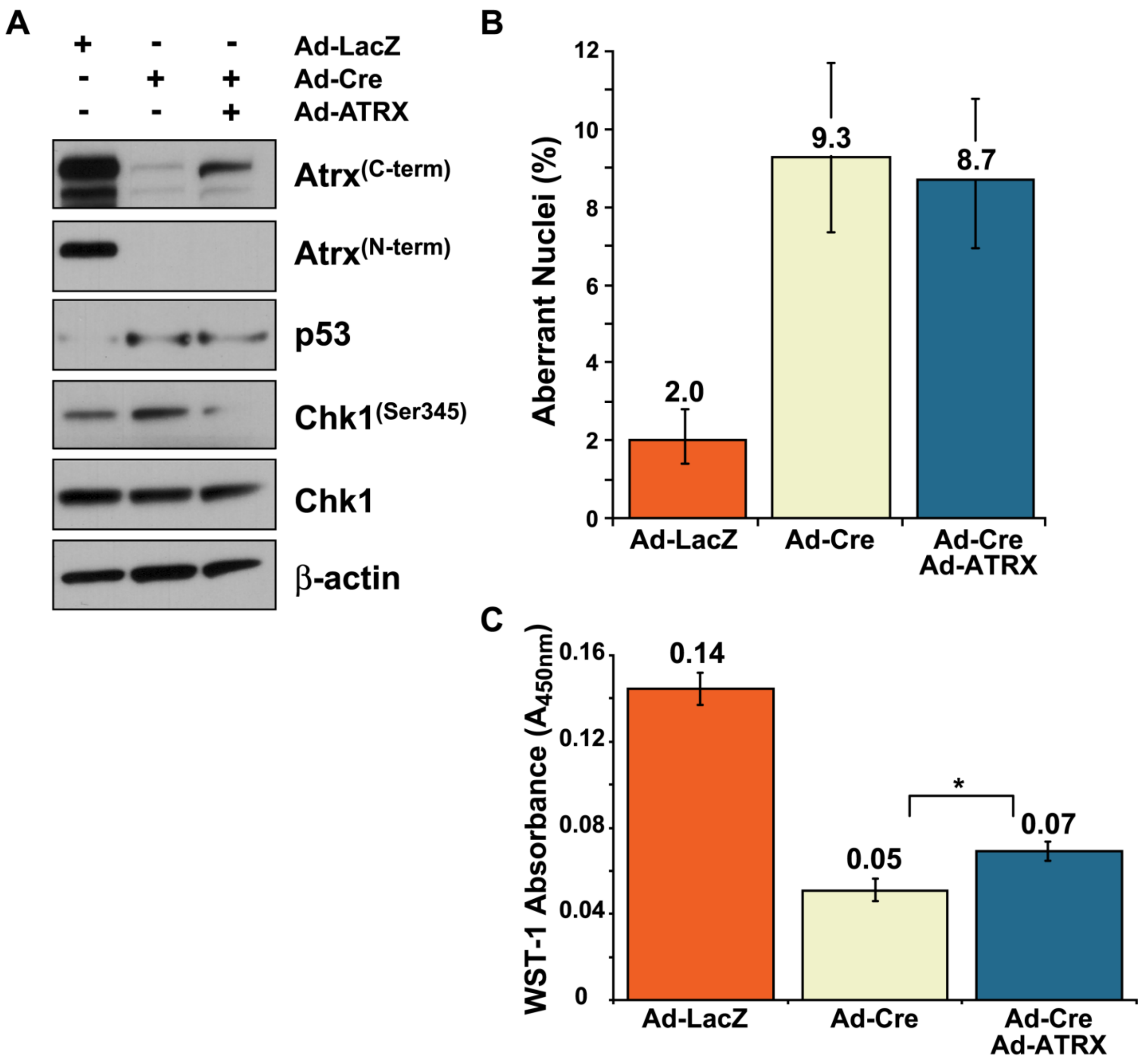

Figure S5. Exogenous re-expression of recombinant ATRX in *Atrx* deleted myoblasts. (A) Western blot analysis of *Atrx*$^{f/y}$ myoblasts infected with Ad-LacZ, Ad-Cre, or by sequential infections of Ad-Cre→Ad-ATRX. Immuno-blots were probed with antibodies that detect exogenous and endogenous Atrx$^{(C\text{-term})}$, endogenous Atrx$^{(N\text{-term})}$, p53, phosphorylated Chk1$^{(Ser345)}$, total Chk1, and β-actin as loading control. (B) Percentage of cells with aberrant nuclei (bi-nucleated, fragmented micro-nuclei, or poly-nuclei) in *Atrx*$^{f/y}$ myoblasts infected with Ad-LacZ, Ad-Cre, or by sequential infections of Ad-Cre →Ad-ATRX. Values represent percent total ± 95% CI. (C) WST-1 proliferation assay. Values represent mean ± SEM (n=4). (*) $p < 0.05$ by t-test.

Table S1. Genotypes of progeny from *Myf5*$^{Cre/+}$ x *Atrx*$^{f/f}$ cross

	Atrx$^{f/y}$	*Atrx*$^{f/y}$: *Myf5-Cre*	*Atrx*$^{f/x}$	*Atrx*$^{f/x}$: *Myf5-Cre*	Total
Viable Pups	38	26	28	43	135
Percent	28.1	19.4	20.7	31.8	100

Table S2. Densitometry quantification of western blots for DNA damage response proteins. Values represent internally normalized fold-changes in Ad-Cre infected *Atrx*$^{f/y}$ myoblasts in growth media (NT) or exposed to replication inhibitor hydroxyurea (HU) relative to Ad-LacZ infected *Atrx*$^{f/y}$ myoblasts.

	NT	HU 1hr	HU 2hr	Mean	SD
pATM$^{(Ser1981)}$	3.8	2.5	3.2	3.2	0.7
pChk1$^{(Ser345)}$	1.5	1.2	1.6	1.5	0.2
p53	1.8	1.7	1.7	1.7	0.1
Rad51	0.2	0.5	0.7	0.5	0.2
γ-H2AX	1.6	1.6	2.5	1.9	0.5

Unedited gel Figure 3B

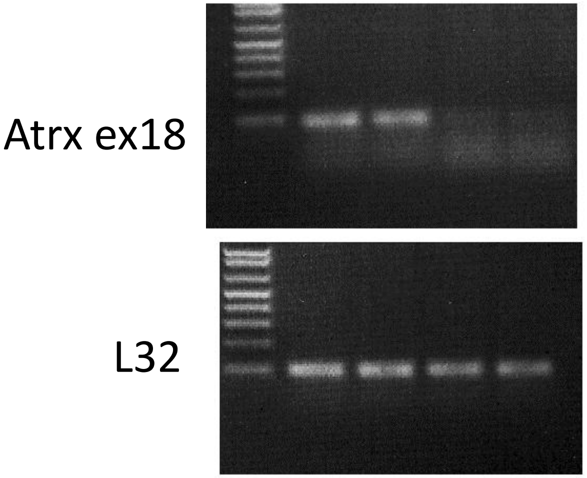

Unedited blot Figure 3C

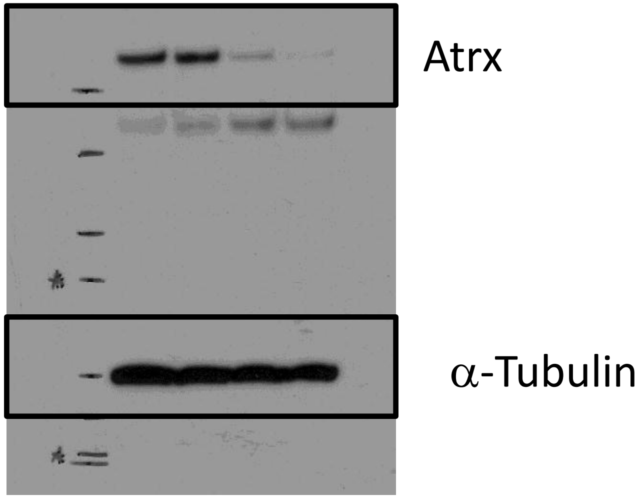

Unedited blot Figure 4A

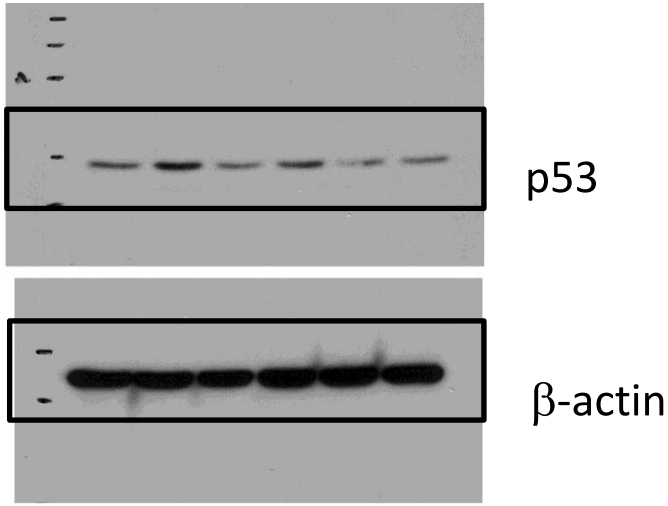

Unedited blot Figure 7A

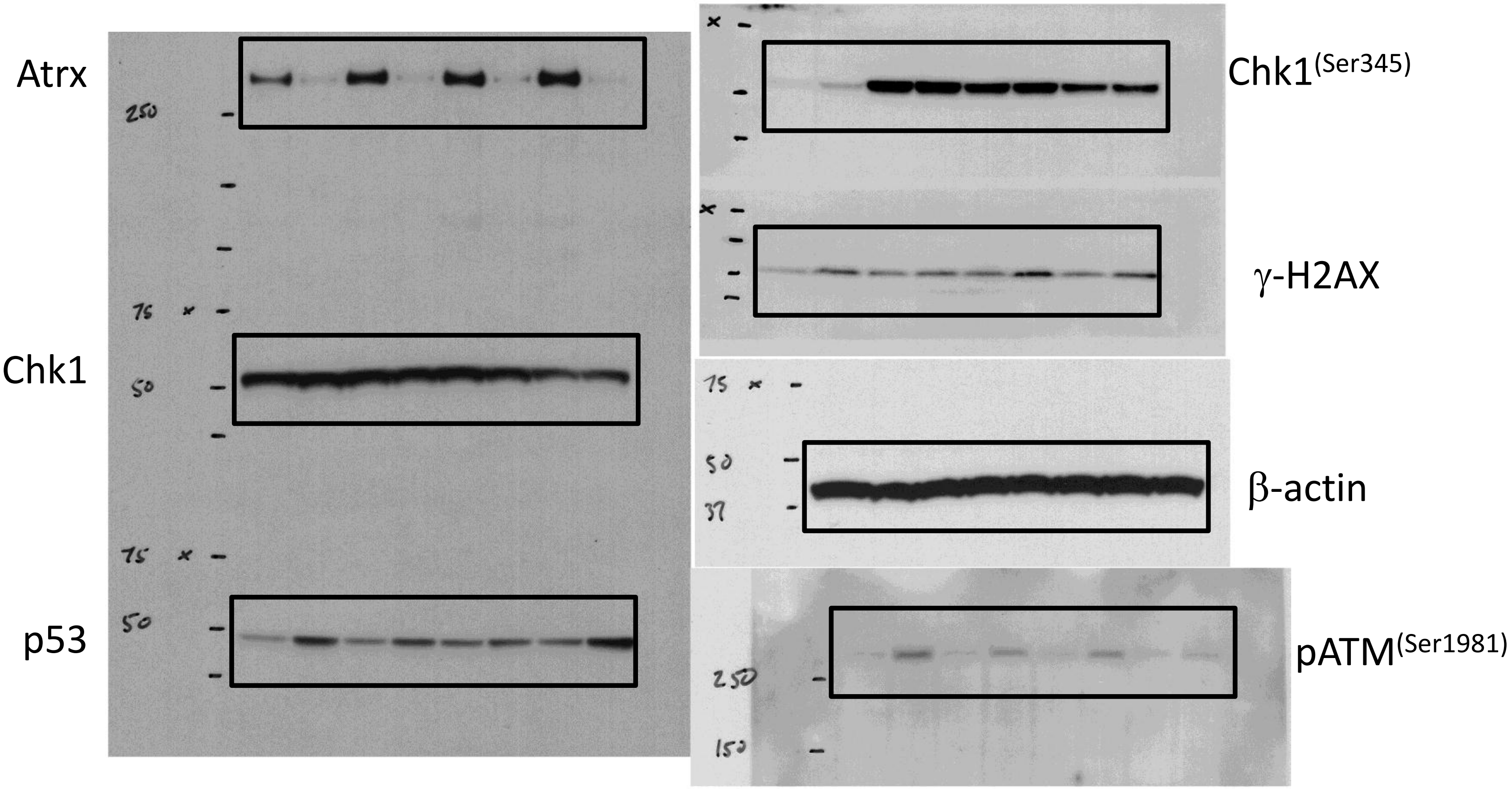

Unedited blot Figure 7B

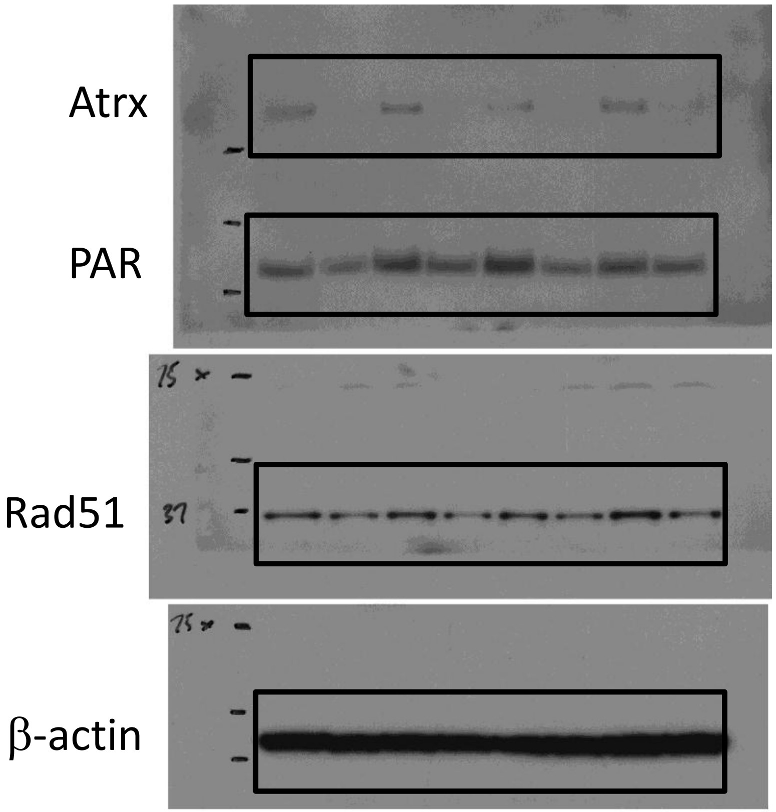

Unedited blot Figure 7C

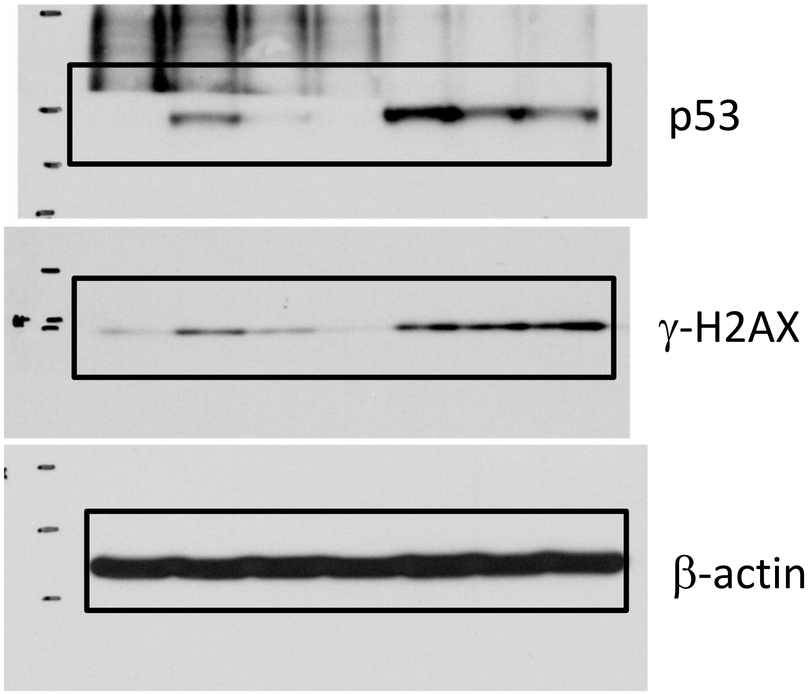

Unedited blot Figure 8B

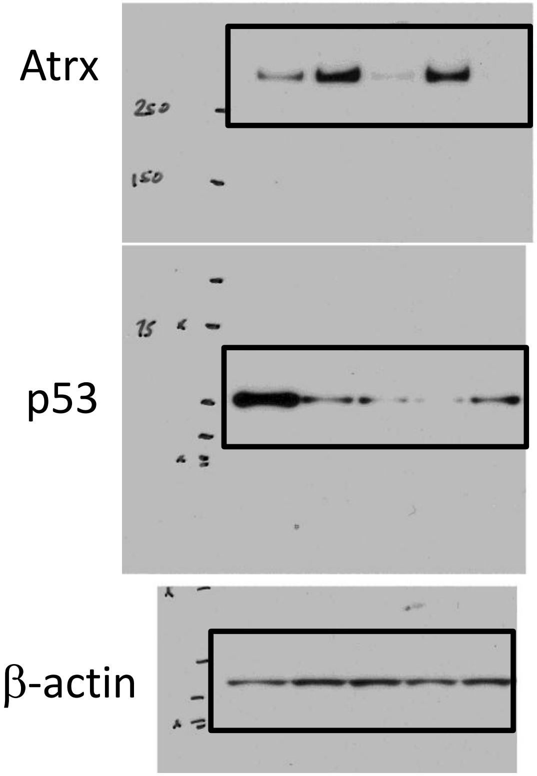

Unedited blot Figure 8D

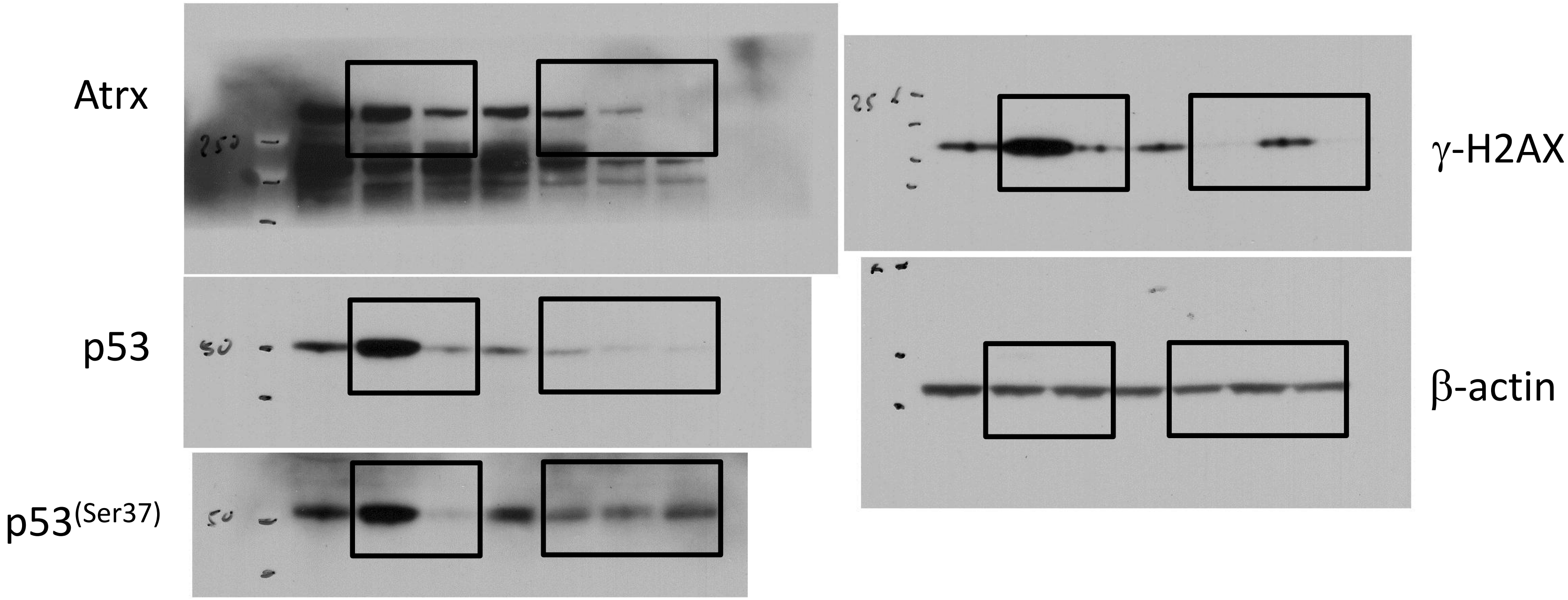

Unedited blot Figure S2B

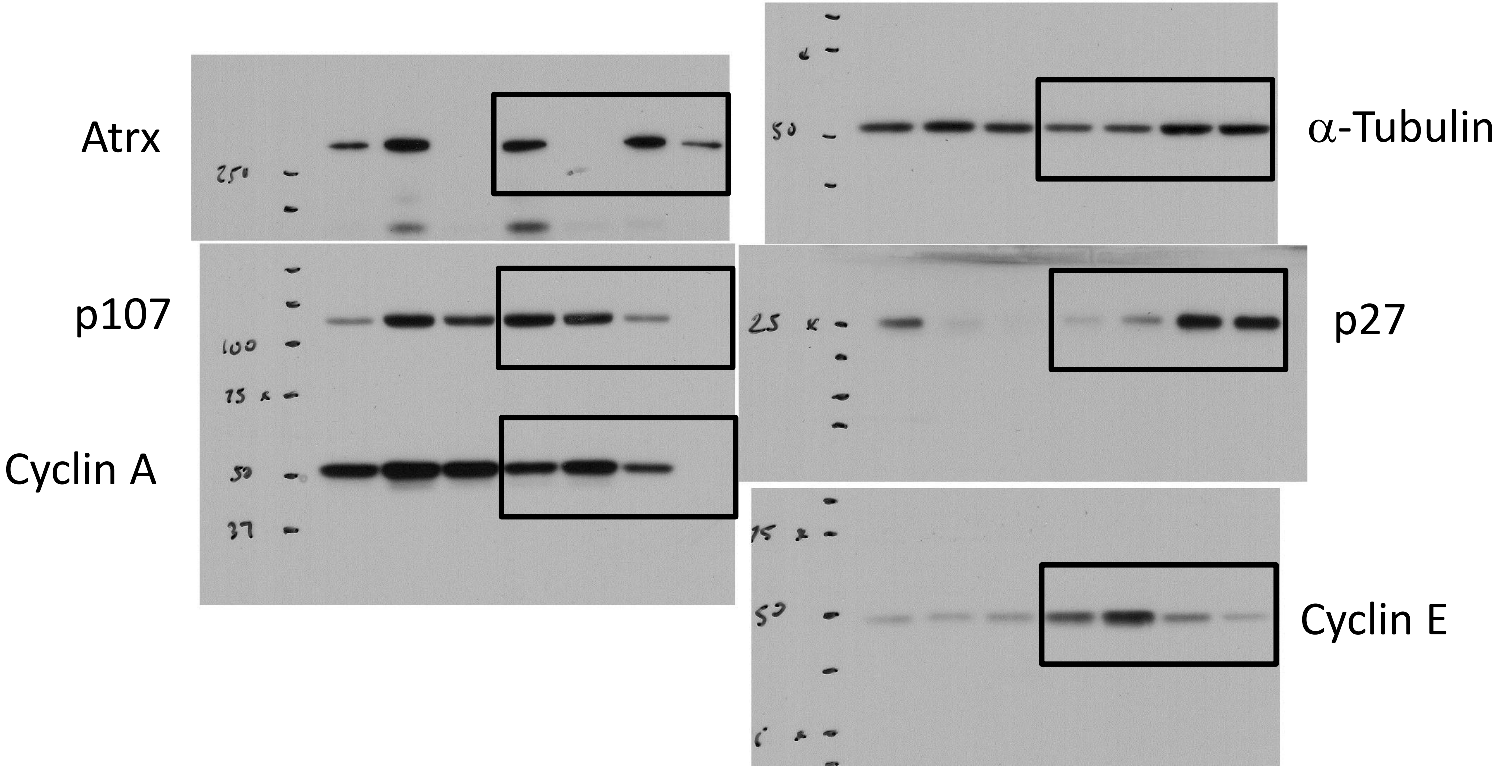

Unedited blot Figure S5A